



HAL
open science

Marine reservoir ages for coastal West Africa

Guillaume Soulet, Philippe Maestrati, Serge Gofas, Germain Bayon, Fabien Dewilde, Maylis Labonne, Bernard Dennielou, Franck Ferraton, Giuseppe Siani

► **To cite this version:**

Guillaume Soulet, Philippe Maestrati, Serge Gofas, Germain Bayon, Fabien Dewilde, et al.. Marine reservoir ages for coastal West Africa. *Geochronology*, 2023, 10.5194/gchron-2023-5 . hal-04420390

HAL Id: hal-04420390

<https://hal.science/hal-04420390v1>

Submitted on 4 Apr 2024

HAL is a multi-disciplinary open access archive for the deposit and dissemination of scientific research documents, whether they are published or not. The documents may come from teaching and research institutions in France or abroad, or from public or private research centers.

L'archive ouverte pluridisciplinaire **HAL**, est destinée au dépôt et à la diffusion de documents scientifiques de niveau recherche, publiés ou non, émanant des établissements d'enseignement et de recherche français ou étrangers, des laboratoires publics ou privés.



Distributed under a Creative Commons Attribution 4.0 International License



Marine reservoir ages for coastal West Africa

Guillaume Soulet¹, Philippe Maestrati², Serge Gofas^{2,3}, Germain Bayon¹, Fabien Dewilde¹, Maylis Labonne⁴, Bernard Dennielou¹, Franck Ferraton⁴, Giuseppe Siani⁵

1 Ifremer, Univ Brest, CNRS, Geo-Ocean UMR6538, F-29280, Plouzané, France

5 2 Muséum National d'Histoire Naturelle, Paris, DGD-Collections, France

3 Departamento de Biología Animal, Facultad de Ciencias, Universidad de Málaga, Málaga, Spain

4 MARBEC, Univ Montpellier, CNRS, Ifremer, IRD, Montpellier, France

5 GEOPS, UMR 8148 Université Paris-Saclay, Orsay, France

Correspondence to: Guillaume Soulet (gsoulet@ifremer.fr)

10 **Abstract.** We measured the ¹⁴C age of pre-bomb suspension-feeding bivalves of known-age from coastal West Africa (n=30)
across a latitudinal transect extending from 33°N to 15°S. The specimens are from the collections of the Muséum National
d'Histoire Naturelle (Paris, France). They were carefully chosen to ensure that the specimens were alive when collected or
died not long before collection. From the ¹⁴C-dating of these know-age bivalves, we calculated the marine reservoir age (as
ΔR and R values) for each specimen. ΔR values were calculated relative to the Marine20 calibration curve and the R values
15 relative to Intcal20 or SHcal20 calibration curves. Except five outliers, the ΔR and R values were quite homogenous to a mean
value of -77 ± 47 ¹⁴C yrs (1sd, n = 25), and of 400 ± 59 ¹⁴C yrs (1sd, n = 25), respectively. These values are typical of low
latitude marine reservoir age values. Five suspension-feeding species living in five different ecological habitats were studied.
For localities where different species were available, the results yielded similar results whatever the species considered
suggesting that the habitat has only a limited impact on the marine reservoir age reconstruction. We show that our measured
20 marine reservoir ages follow the declining trend of the global marine reservoir age starting ca. 1900 AD, suggesting that marine
reservoir age of coastal West Africa is driven, at least at first order, by the global carbon cycle and climate rather than by local
effects. Each outlier was discussed. Sub-fossil specimens likely explain the older ¹⁴C age and thus larger marine reservoir age
measured for these samples. *Bucardium ringens* might not be a best choice for marine reservoir age reconstructions.

1 Introduction

25 The marine reservoir age (R) at a given calendar time/year (t) is the difference between the radiocarbon age (¹⁴C) of the
dissolved inorganic carbon (DIC) of the ocean (¹⁴C_m) and that of atmospheric CO₂ (¹⁴C_{atm}) (Stuiver and Polach, 1977; Ascough
et al., 2005; Soulet et al., 2016; Skinner and Bard, 2022; Soulet, 2015):

$$R(t) = {}^{14}\text{C}_m(t) - {}^{14}\text{C}_{\text{atm}}(t) \quad (1)$$

At global scale, the marine reservoir age of the surface mixed layer of the ocean is set by the exchange of “young” CO₂ at the
30 atmosphere-ocean interface, plus the exchange of DIC between oceanic surface waters and deep waters that contain large



amounts of “old” DIC (Bard, 1988; Skinner and Bard, 2022). The ^{14}C age of the global ocean over time, i.e., the Marine20 calibration curve (Heaton et al., 2020), has been modelled using the global carbon cycle box model BICYCLE (Köhler et al., 2006; Köhler and Fischer, 2006, 2004; Köhler et al., 2005) and the Northern Hemisphere atmospheric ^{14}C calibration curve (IntCal20; Reimer et al., 2020). While the global marine calibration curve (Marine20) is widely used to derive calibrated ages from ^{14}C dating of marine samples, it does not account for local marine ^{14}C offsets due to, for instance, continental carbon inputs to the coastal ocean, regional winds, and changes in the oceanic circulation and climate (Bard, 1988; Alves et al., 2018; Skinner and Bard, 2022; Heaton et al., 2023). Hence, the usefulness of the ΔR metric (Stuiver et al., 1986; Stuiver and Braziunas, 1993; Reimer and Reimer, 2017) that is the difference between the ^{14}C age of any marine sample ($^{14}\text{C}_m$) and that of the marine calibration curve ($^{14}\text{C}_{\text{Marine20}}$) at the same time (t):

$$\Delta R(t) = {}^{14}\text{C}_m(t) - {}^{14}\text{C}_{\text{Marine20}}(t) \quad (2)$$

The local marine reservoir age offset (ΔR) is known to vary largely as demonstrated by pre-bomb values ranging between – 500 to + 2000 ^{14}C years (Reimer and Reimer, 2001) depending on the location. Larger ΔR values are located at high-latitudes while values close to $\Delta R = 0$ ^{14}C years are located at low latitudes (Bard, 1988; Bard et al., 1994).

From a geochronological perspective (i.e., calibration of marine ^{14}C dates and building age-depth model from marine ^{14}C dates), knowing $\Delta R(t)$ is of crucial interest to correct marine ^{14}C dates for a local ^{14}C offset compared to the global marine calibration curve and hence a pre-requirement to derive accurate calendar ages. Reconstructing $\Delta R(t)$ values from unstudied areas is also valuable as it could contribute to deriving regional/local marine calibration curves from the global one using 3-D large-scale ocean circulation model (Butzin et al., 2017; Alves et al., 2019).

From a carbon cycle perspective, the $R(t)$ and $\Delta R(t)$ are also very important as they reflect ^{14}C disequilibria between the ocean and the atmosphere and hence they are key proxies to understand local variations of the global carbon cycle, and its evolution over time with changing climate and environment (Skinner et al., 2015, 2010; Lindsay et al., 2016; Soulet et al., 2011; Siani et al., 2001; Schefuß et al., 2016; Heaton et al., 2021).

On a whole, efforts to estimate $R(t)$ and $\Delta R(t)$ values wherever possible are valuable to the understanding of both modern and past carbon cycle, and the reconstruction of climate and environmental changes based on sedimentary archives.

Pre-bomb $R(t)$ and $\Delta R(t)$ values for coastal West Africa are very sparse. According to the Marine Reservoir Correction Database (Reimer and Reimer, 2001; <http://calib.org/marine/>; last seen 15/11/2022), from Oran on the Mediterranean coast of Algeria (Siani et al., 2000) to Hondelkip Bay on the Atlantic coast of South Africa (Dewar et al., 2012), only few marine reservoir ages from Mauritania and Senegal were reported (Ndeye, 2008) (Fig. 1). For Mauritania, collection sites were Nouadhibou (formerly Port-Étienne, 2 samples), the area of the Cape Timiris – El Mamghar (3 samples). Two samples were collected from an unknown location from coastal Mauritania. For Senegal, collection sites were restricted to the Dakar area (Almadies, Dakar harbour, Gorée Island and Rufisque; 5 samples). Thirteen additional samples were from unknown locations from coastal Senegal.

In this study we report new marine reservoir age values ($n=30$) based on the ^{14}C dating of bivalves with a known pre-bomb collection date and collected across a latitudinal transect extending from Mohammedia (Morocco, 33°N) to Moçâmedes



65 (Angola, 15°S). Our suite of sample includes specimens from Mauritania, Senegal, Republic of Guinea, Sierra Leone, Ivory
Coast, Benin, Gabon and Republic of Congo (Fig. 1, Table S1 in the Supplement). We used specimens of five different species:
Senilia senilis, *Bucardium ringens*, *Donax rugosus*, *Ostrea stentina* and *Pseudochama gryphina*. We briefly discuss our results
in the context of local environmental setting of the studied bivalves and regional oceanography of the Eastern Atlantic Ocean.

2 Material and methods

70 2.1 Material

Bivalve shells were selected from the collections of the Muséum National d'Histoire Naturelle (MNHN) (Paris, France). We
carefully chose pre-bomb specimens of known-age and ensured that they were collected alive or very soon after death. For
example, specimens with articulated valves and exhibiting flesh remains inside the shell were clearly collected alive. For
Senilia senilis, the presence of the fragile periostracum provides evidence that the specimen was collected fresh. For *Bucardium*
75 *ringens*, remains of the hinge ligament indicate that the bivalve death occurred not long before collection. The collection date
was also carefully checked. Below, we provide background information for the five different bivalve species investigated in
this study. Additional information for each sample is given in section 3.1.

Senilia senilis (Linnaeus, 1758) can be found from Mauritania to northern Angola. It lives in fine sand in estuaries, creeks or
lagoon with regular tidal influence from the lower intertidal zone to about 2 meters water depth. The specie is tolerant to
80 seasonal salinity changes (von Cosel and Gofas, 2019). *S. senilis* is a suspension feeder that lives in the top 5-10-cm layer of
the sediment (Okera, 1976; Catry et al., 2017).

Bucardium ringens (Bruguière, 1789) occurs from Mauritania to southern Angola. It lives in clean fine sand and mixed sand
on open coast from shallow (5-10 meters depth) to about 50 meters depth. Shells and valves are commonly cast ashore on
beaches but live-taken specimens are rare (von Cosel and Gofas, 2019). *B. ringens* is likely a suspension feeder as typically
85 are cardiids (Herrera et al., 2015).

Donax rugosus (Linnaeus, 1758) occurs from Mauritania to Ghana and from northern Angola to southern Angola. It lives in
mixed and coarse sand in the surf zone of open beaches (von Cosel and Gofas, 2019). *D. rugosus* is a suspension feeder (Smith,
1971).

Ostrea stentina (Payraudeau, 1826) can be found southern Portugal to Ghana, then from Gabon to northern Angola. It is
90 common and occurs on various types of hard substrate such as rocks, stones, pebbles and other oysters from 1 to 30 meters
depths. It can also be found in lagoons, inlets and creeks under marine condition (von Cosel and Gofas, 2019). *O. stentina* is a
suspension feeder (Türkmen et al., 2005).

Pseudochama gryphina (Lamarck, 1819) occurs from Southern Portugal to Mauritania and from Gabon to southern Angola
(von Cosel and Gofas, 2019) and lives on hard substrate such as rocks and stones in clear water offshore about 10 to 60 meters
95 water depth. *P. gryphina* is a suspension feeder (Sessa et al., 2013).



A small piece (30-100 mg) of the outermost layers of each shell was cut using a Dremel™ rotary tool fitted with a cut-off wheel. We focused on the external part of the shell to ensure that we sampled and dated the most recent part (likely the last few months) of the specimen. The shell carbonate samples were then sonicated and rinsed in deionized water at least 5 times. Samples were coarsely crushed and split into a subsample for stable isotopic analysis and a subsample for ^{14}C analysis.

100 2.2 Radiocarbon measurements

Samples were washed with dilute HNO_3 (0.01M) for 15 min then rinsed to neutral pH. Then the shell carbonate was converted into CO_2 following LMC14 laboratory (Laboratoire de Mesure du Radiocarbone, Saclay, France) standard phosphoric acid hydrolysis procedure (Tisnérat-Laborde et al., 2001; Dumoulin et al., 2017). The CO_2 was then converted to graphite (Cottreau et al., 2007; Dumoulin et al., 2017) and analyzed for its ^{14}C composition by Accelerator Mass Spectrometry (AMS) using the Artémis ^{14}C AMS facility (Moreau et al., 2013). Results are corrected for the $^{13}\text{C}/^{12}\text{C}$ ratio as measured on the AMS (Santos et al., 2007) and are reported in the $F^{14}\text{C}$ notation (Reimer et al., 2004). $F^{14}\text{C}$ is identical to the $A_{\text{SN}}/A_{\text{ON}}$ metric (Stuiver and Polach, 1977), and the $^{14}\text{a}_\text{N}$ notation (Mook and van der Plicht, 1999). Corresponding conventional ^{14}C ages reported in ^{14}C years Before Present (AD 1950) were calculated according to:

$$^{14}\text{C} = -8033 \ln(F^{14}\text{C}) \quad (3)$$

110 2.3 Stable carbon isotopes

Stable carbon and oxygen isotopic analyses of the dated samples were performed at the Pôle Spectrométrie Océan (PSO, Plouzané, France) using a MAT-253 (Thermo Scientific) stable isotope ratio mass spectrometer (IRMS) coupled with a Kiel IV Carbonate Device (Thermo Scientific). The measurements are reported versus Vienna Pee Dee Belemnite standard (VPDB) defined with respect to two international carbonate standards: NBS-19 ($\delta^{18}\text{O} = -2.20 \text{ ‰}$ and $\delta^{13}\text{C} = +1.95 \text{ ‰}$) and NBS-18 ($\delta^{18}\text{O} = -23.20 \text{ ‰}$ and $\delta^{13}\text{C} = -5.01 \text{ ‰}$). The mean external reproducibilities (1σ), based on repeated measurements of an in-house standard, was $\pm 0.04 \text{ ‰}$ and $\pm 0.02 \text{ ‰}$ for $\delta^{18}\text{O}$ and $\delta^{13}\text{C}$ values, respectively.

2.4 Marine Reservoir Age calculation

The marine reservoir age R of the selected shells is calculated according to equation (1) where t is the collection year as known from the museum records (Table S1 in the Supplement and section results), $^{14}\text{C}_m$ is the measured shell ^{14}C age, and $^{14}\text{C}_{\text{atm}}$ is the ^{14}C age of the atmosphere. For shells picked from the northern hemisphere, $^{14}\text{C}_{\text{atm}}$ is obtained from the IntCal20 calibration curve (Reimer et al., 2020). For shells from the southern hemisphere, we used instead the southern hemisphere calibration curve SHCal20 (Hogg et al., 2020). The uncertainty is calculated (Soulet, 2015) according to:

$$\sigma_{R(t)} = \sqrt{\sigma_{^{14}\text{C}_m(t)}^2 + \sigma_{^{14}\text{C}_{\text{atm}}(t)}^2} \quad (4)$$

Note that mean SHCal20 offset compared to IntCal20 is estimated to be 36 ± 27 ^{14}C yrs. Thus, the R values calculated with IntCal20 or SHcal20 are essentially the same if one take uncertainties into account.



The local marine reservoir offset ΔR of the selected shells is calculated according to equation (2) where t is the collection year as known from the museum records (Table S1 in the Supplement and section results), $^{14}\text{C}_m$ is the measured shell ^{14}C age, and $^{14}\text{C}_{\text{Marine20}}$ is the ^{14}C age of the global marine calibration curve. The uncertainty is calculated as follows:

$$\sigma_{\Delta R(t)} = \sqrt{\sigma_{^{14}\text{C}_m(t)}^2 + \sigma_{^{14}\text{C}_{\text{Marine20}}(t)}^2} \quad (5)$$

130 Note that Reimer and Reimer (2017) do not propagate the uncertainty of Marine20 calibration curve.

3 Results and Discussion

3.1 Radiocarbon measurements results

The results are shown in Table S1 in the Supplement. Below we provide the detailed list of the samples used in this study. We classified the samples by location with corresponding geographic coordinates, then by species. Code numbers “MNHN-IM-2022-xxxx” allows one to find the samples in the collections of the MNHN of Paris (France). Code numbers “SacA-xxxxx” are the radiocarbon laboratory number for the sample.

3.1.1 Samples from Morocco

MNHN-IM-2022-4615

Ostrea stentina

140 Mohammedia (33.71°N, 7.37°W)

Articulated specimen with remains of flesh.

SacA-68834: 482 ± 18 BP

$F^{14}\text{C} = 0.9418 \pm 0.0021$

$\delta^{13}\text{C} = 1.19 \text{ ‰ VPDB}$

145 Collection date: 1921

Collector: Jacques de Lépiney

Museum label: *Ostrea stentina* Payr, Fedhala 1921, donat J de Lépiney 1939

MNHN-IM-2022-4609

150 *Ostrea stentina*

El Jadida, beach (33.25°N, 8.49°W)

An isolated valve looking quite fresh.

SacA-68828: 817 ± 18 BP

$F^{14}\text{C} = 0.9033 \pm 0.0020$

155 $\delta^{13}\text{C} = 0.71 \text{ ‰ VPDB}$



Collection date: October 26th 1909

Collector: Louis Gentil

Museum label: Plage de Mazagan 26 octobre 1909, Maroc, Louis Gentil

160 MNHN-IM-2022-4608

Ostrea stentina

Lagoon of Sidi Moussa (32.98°N, 8.75°W)

Articulated specimen with remains of flesh.

SacA-68827: 1058 ± 19 BP

165 F¹⁴C = 0.8766 ± 0.0021

δ¹³C = -0.48 ‰ VPDB

Collection date: 1924

Collector: Jacques de Lépiney

Museum label: *Ostrea stentina* Payr., lagune de Sidi Moussa (région de Mazagan), 1924, donat. J de Lépiney 1939

170 **3.1.2 Samples from Mauritania**

MNHN-IM-2022-4612

Ostrea stentina

Nouadhibou, Pointe Chacal (20.91°N, 17.04°W)

Articulated specimen.

175 SacA-68831: 514 ± 17 BP

F¹⁴C = 0.9381 ± 0.0020

δ¹³C = 2.28 ‰ VPDB

Collection date: 1948

Collector: Roger Sourie

180 Museum label: Port Etienne (Pointe des Chacals) M. Sourie, 1948

MNHN-IM-2022-4610

Ostrea stentina

Cansado Bay (20.88°N, 17.04°W)

185 Articulated specimen with remains of flesh.

SacA-68829: 516 ± 17 BP

F¹⁴C = 0.9378 ± 0.0020



$\delta^{13}\text{C} = 2.09 \text{ ‰ VPDB}$

Collection date: 1911-1912

190 Collector: Mission Gruvel

Museum label: *Ostrea stentina* Payr. = *lacerans* Hanl., Baie de Cansado, Mission Gruvel, 1911-1912

MNHN-IM-2022-4599

Bucardium ringens

195 Nouadhibou (20.88°N, 17.04°W)

An isolated valve of a juvenile with remains of the hinge ligament.

SacA-68811: $863 \pm 18 \text{ BP}$

$F^{14}\text{C} = 0.8981 \pm 0.0020$

$\delta^{13}\text{C} = 0.38 \text{ ‰ VPDB}$

200 Collection date: 1908

Collector: Mission Gruvel

Museum label: *Cardium ringens* Gmelin; Port Etienne; 1908; Mission Gruvel

MNHN-IM-2022-4603

205 *Donax rugosus*

Ndiago, beach (16.17°N, 16.51°W)

Articulated specimen with remains of flesh and hinge ligament.

SacA-68815: $518 \pm 19 \text{ BP}$

$F^{14}\text{C} = 0.9376 \pm 0.0022$

210 $\delta^{13}\text{C} = 0.68 \text{ ‰ VPDB}$

Collection date: January 21st 1908

Collector: Mission Gruvel

Museum label: *Donax rugosus* Linné, N'Diago plage, 21.I.08, Mission Gruvel

3.1.3 Samples from Senegal

215 MNHN-IM-2022-4607

Donax rugosus

Saint Louis (16.02°N, 16.51°W)

Articulated specimen with remains of flesh and hinge ligament.

SacA-68819: $574 \pm 18 \text{ BP}$

220 $F^{14}\text{C} = 0.9310 \pm 0.0021$



$\delta^{13}\text{C} = 1.29 \text{‰ VPDB}$

Collection date: December 1901

Collector: Buchet's mission

Museum label: Sénégal, Saint Louis, Coquilles; Donax, M^{on} Buchet, X^{bre} 1901

225

MNHN-IM-2022-4592

Senilia senilis

Dakar, backwaters of the "Marigot de Hann" (14.74°N, 17.39°W)

Articulated specimen with remains of flesh and well-preserved periostracum.

230 SacA-68824: 560 ± 17 BP

$F^{14}\text{C} = 0.9327 \pm 0.0020$

$\delta^{13}\text{C} = -0.29 \text{‰ VPDB}$

Collection date: May 1908

Collector: Mission Gruvel

235 Museum label: Arca (*Senilia*) *senilis* Linné, Marigot de Hann V.1908, se vend sur le marché de Dakar env. 2 sous la douzaine, Mission Gruvel

Note: The Marigot of Hann seems to have been a creek more or less connected to the ocean. It was drawn on a map of Dakar in 1905 but does not exist any longer. The map can be accessed from the Gallica website managed by the Bibliothèque Nationale de France: <https://gallica.bnf.fr/ark:/12148/btv1b53197802m>

240

MNHN-IM-2022-4593

Senilia senilis

Dakar, Bay of Hann, Pointe Bel Air, beach at low tide (14.71°N, 17.42°W)

Articulated specimen with remains of flesh and well-preserved periostracum.

245 SacA-68825: 544 ± 18 BP

$F^{14}\text{C} = 0.9346 \pm 0.0020$

$\delta^{13}\text{C} = 0.07 \text{‰ VPDB}$

Collection date: December 1st 1909

Collector: Mission Gruvel

250 Museum label: Arca (*Senilia*) *senilis* Linné, Baie de Hann, Pointe de Bel Air, plage à basse mer, M Gruvel, 1.XII.1909

MNHN-IM-2022-4606

Donax rugosus

Dakar, Bay of Hann (14.71°N, 17.42°W)



255 Articulated specimen with remains of flesh and hinge ligament.

SacA-68818: 526 ± 18 BP

$F^{14}C = 0.9366 \pm 0.0022$

$\delta^{13}C = 0.33$ ‰ VPDB

Collection date: April 1908

260 Collector: Mission Gruvel

Museum label: *Donax rugosus* Linné, Baie de Hann à basse mer, IV 08, Mission Gruvel

MNHN-IM-2022-4598

Bucardium ringens

265 Dakar, Bay of Hann at low tide (14.71°N, 17.42°W)

An isolated valve with remains of the hinge ligament.

SacA-68810: 628 ± 17 BP

$F^{14}C = 0.9247 \pm 0.0019$

$\delta^{13}C = 0.68$ ‰ VPDB

270 Collection date: April 1908

Collector: Mission Gruvel

Museum label: *Cardium ringens* Gmelin, Baie de Hann à basse mer, IV.08, Mission Gruvel

MNHN-IM-2022-4616

275 *Ostrea stentina*

Dakar, beach of Hann, posts of the pontoon (14.71°N, 17.42°W)

An isolated valve with remains of flesh

SacA-68835: 539 ± 19 BP

$F^{14}C = 0.9351 \pm 0.0022$

280 $\delta^{13}C = 1.56$ ‰ VPDB

Collection date: 1947

Collector: Roger Sourie

Museum label: *Ostrea stentina* Payr Dakar (plage de Hann, piles du ponton) M Sourie 1947

3.1.4 Samples from Republic of Guinea

285 MNHN-IM-2022-4601

Bucardium ringens

Los Islands, Roume Island at low tide (9.46°N, 13.79°W)



A fresh-looking isolated valve.

SacA-68813: 857 ± 39 BP

290 $F^{14}C = 0.8988 \pm 0.0043$

$\delta^{13}C = -0.40$ ‰ VPDB

Collection date: December 20th 1909

Collector: Mission Gruvel

Museum label: *Cardium ringens* Gmelin; Ile Roumé, archipel de Los, à basse mer, 20.XII.09, Mission Gruvel

295

MNHN-IM-2022-4618

Pseudochama gryphina

Los Islands, Tamara Island (9.46°N, 13.83°W)

An articulated specimen.

300 SacA-68820: 502 ± 19 BP

$F^{14}C = 0.9395 \pm 0.0022$

$\delta^{13}C = 1.52$ ‰ VPDB

Collection date: 1909-1910

Collector: Mission Gruvel

305 Museum label: *Chama gryphina* Lm, Tamara, Guinée, mission Gruvel, 1909-1910

Note: It is possible that this sample was also collected in December 1909 as sample MNHN-IM-2022-4601

3.1.5 Sample from Sierra Leone

MNHN-IM-2022-4611

Ostrea stentina

310 Near Cape Saint Ann (7.56°N, 12.94°W)

Articulated specimen with remains of flesh.

SacA-68830: 464 ± 18 BP

$F^{14}C = 0.9439 \pm 0.0021$

$\delta^{13}C = 1.04$ ‰ VPDB

315 Collection date: 1912

Collector: Mission Gruvel

Museum label: Sierra Léone près Cap Ste Anne, m. Gruvel, 1912

3.1.6 Samples from Benin

MNHN-IM-2022-4591



- 320 *Senilia senilis*
Ahémé Lake (6.42°N, 1.96°E)
Articulated specimen with well-preserved periostracum
SacA-68823: 414 ± 18 BP
 $F^{14}C = 0.9498 \pm 0.0021$
325 $\delta^{13}C = -4.76$ ‰ VPDB
Collection date: February 1910
Collector: Mission Gruvel
Museum label: Arca (*Senilia*) *senilis* Linné, Lac Ahémé Dahomey, Mission Gruvel, II.1910
- 330 MNHN-IM-2022-4600
Bucardium ringens
Cotonou, dredging at a water depth of 20-25 meters (6.33°N, 2.39°E)
A fresh isolated valve of a juvenile.
SacA-68812: 606 ± 18 BP
335 $F^{14}C = 0.9273 \pm 0.0020$
 $\delta^{13}C = 0.26$ ‰ VPDB
Collection date: February 1910
Collector: Mission Gruvel
Museum label: *Cardium ringens*, Cotonou, mer, II.1910, sac 372, Mission Gruvel
- 340 Note: The information that the sample came from a dredging at 20-25 meters water depth in front of Cotonou can be found in Dautzenberg (1912).

MNHN-IM-2022-4602
Bucardium ringens
345 La Bouche du Roi, Grand Popo, beach (6.29°N, 1.92°E)
An isolated valve with remains of the hinge ligament.
SacA-68814: 527 ± 17 BP
 $F^{14}C = 0.9365 \pm 0.0020$
 $\delta^{13}C = 0.25$ ‰ VPDB
350 Collection date: February 1910
Collector: Mission Gruvel
Museum label: *Cardium ringens* Gmelin, Bouche du Roi, Gd Popo, plage, II.1910, Mission Gruvel.



Note: Three labels mention the same location, but one label mentions the Catumbella estuary (Angola, June 17th 1910). We believe the sample is from Grand Popo.

355 3.1.7 Samples from Ivory Coast

MNHN-IM-2022-4595

Bucardium ringens

Grand Bassam, beach (5.19°N, 3.73°W)

An isolated valve with remains of the hinge ligament.

360 SacA-68807: 507 ± 18 BP

$F^{14}C = 0.9388 \pm 0.0021$

$\delta^{13}C = 0.29 \text{ ‰ VPDB}$

Collection date: 1909-1910

Collector: Mission Gruvel

365 Museum label: *Cardium ringens* Gmelin, plage de Gd Bassam 1909-10, mission Gruvel.

MNHN-IM-2022-4597

Bucardium ringens

Jacquerville, beach (5.19°N, 4.42°W)

370 An isolated valve of a juvenile with remains of the hinge ligament.

SacA-68809: 995 ± 18 BP

$F^{14}C = 0.8835 \pm 0.0020$

$\delta^{13}C = 0.03 \text{ ‰ VPDB}$

Collection date: January 10th 1910

375 Collector: Mission Gruvel

Museum label: *Cardium ringens* Gmel., Jacquerville Côte d'Ivoire, plage, 19.I.10, Mission Gruvel.

3.1.8 Sample from Gabon

MNHN-IM-2022-4613

Ostrea stentina

380 Port-Gentil (0.71°S, 8.79°E)

An isolated valve with remains of flesh.

SacA-68832: 497 ± 19 BP

$F^{14}C = 0.9401 \pm 0.0022$

$\delta^{13}C = 2.24 \text{ ‰ VPDB}$



385 Collection date: 1948

Collector: Charles Roux' mission

Museum label: Port Gentil, M Roux, 1949.

Note: Charles Roux writes in 1949 (Roux, 1949) that he was in the Port-Gentil area during the year 1948. We can understand that he was already back to France in 1949. Hence, the collection date must be 1948.

390 3.1.9 Samples from Republic of Congo

MNHN-IM-2022-4614

Ostrea stentina

Loango (4.66°S, 11.80°E)

An isolated valve with remains of flesh.

395 SacA-68833: 571 ± 19 BP

$F^{14}\text{C} = 0.9314 \pm 0.0022$

$\delta^{13}\text{C} = 1.38 \text{‰ VPDB}$

Collection date: 1890

Collector: Augusto Nobre

400 Museum label: *Ostrea stentina* Payr Loango M. Nobre 1890

MNHN-IM-2022-4604

Donax rugosus

Pointe-Noire (4.76°S, 11.84°E)

405 A fresh isolated valve from a juvenile specimen.

SacA-68816: 447 ± 18 BP

$F^{14}\text{C} = 0.9459 \pm 0.0021$

$\delta^{13}\text{C} = 0.84 \text{‰ VPDB}$

Collection date: December 1936 – April 1937

410 Collector: Edgard Aubert de la Rüe

Museum label: Pte Noire, Aubert de la Rüe, 1937

Note: Edgard Aubert de la Rüe was in Congo from 18/12/1936 to 16/04/1937 as evidences by his field books kept in the archives of the Musée du Quai Branly (files 2AP/62 to 2AP/64)

3.1.10 Samples from Angola

415 MNHN-IM-2022-4590

Senilia senilis



Cabinda (5.55°S, 12.20°E)

Articulated specimen with well-preserved periostracum.

SacA-68822: 584 ± 17 BP

420 $F^{14}C = 0.9298 \pm 0.0020$

$\delta^{13}C = -1.15$ ‰ VPDB

Collection date: 1885-1887

Collector: Paul Hesse

Museum label: Cabinda, Cabinda, Angola; C.R. Boettger coll. 1909

425 Note: The shell was donated by Caesar R. Boettger to the MNHN in 1909 (Oliver and von Cosel, 1992) but collected earlier by Paul Hesse when Hesse was leaving in Banana (Democratic Republic of Congo) south of Cabinda (Boettger, 1912). Boettger (1912, p. 110) writes that Hesse's collection includes a number of *Senilia senilis* specimens from Cabinda. The collection date is unfortunately not provided. However, Hesse was employed by a trading company in Banana by the end/beginning 1884/1885 since at least after March 1886 (Westhoff, 1886). Mollusc specimens reported in Boettger (1912)
430 were collected by Hesse between 1885 and 1886. Also, Hesse collected reptile specimens in Cabinda in 1885 and 1887 (Boettger, 1898). Thus, we believe that the MNHN specimen must have been collected between 1885 and 1887.

MNHN-IM-2022-4594

Senilia senilis

435 Cabinda (5.55°S, 12.20°E)

An isolated valve with well-preserved periostracum.

SacA-68826: 536 ± 19 BP

$F^{14}C = 0.9355 \pm 0.0022$

$\delta^{13}C = -3.11$ ‰ VPDB

440 Collection date: June 6th 1921

Collector: Unknown

Museum label [Stadt collection]: *Arca senilis* Lin, Cabenda, Africa, Guinea, bought just over 1d on June 6th 1921 in Grays Jun rd, (some of the specimens at B. M. are more than double the size of mine).

445 MNHN-IM-2022-4589

Senilia senilis

Luanda, beach (8.78°S, 13.27°E)

Articulated specimen with well-preserved periostracum.

SacA-68821: 538 ± 19 BP

450 $F^{14}C = 0.9353 \pm 0.0022$



$\delta^{13}\text{C} = -0.16 \text{ ‰ VPDB}$

Collection date: May 18th 1910

Collector: Mission Gruvel

Museum label: Arca (*Senilia*) *senilis* Linné, St Paul de Loanda, plage, Mission Gruvel, 18.V.1910.

455

MNHN-IM-2022-4605

Donax rugosus

Luanda, beach (8.82°S, 13.21°E)

Articulated specimen with remains of flesh and hinge ligament.

460 SacA-68817: $528 \pm 18 \text{ BP}$

$F^{14}\text{C} = 0.9364 \pm 0.0021$

$\delta^{13}\text{C} = 0.82 \text{ ‰ VPDB}$

Collection date: May 18th 1910

Collector: Mission Gruvel

465 Museum label: *Donax rugosus* Linné, St Paul de Loanda plage, 18.V.10, Mission Gruvel.

MNHN-IM-2022-4596

Bucardium ringens

Bay of Lobito, near the peninsula (12.33°S, 13.56°E)

470 An isolated valve.

SacA-68808: $595 \pm 17 \text{ BP}$

$F^{14}\text{C} = 0.9286 \pm 0.0020$

$\delta^{13}\text{C} = 1.51 \text{ ‰ VPDB}$

Collection date: June 1910

475 Collector: Mission Gruvel

Museum label: *Cardium ringens* Gmelin, Baie de Lobito côté presqu'île, VI.1910, mission Gruvel.

MNHN-IM-2022-4617

Ostrea stentina

480 Moçâmedes (15.18°S, 12.14°E)

A fresh isolated valve.

SacA-68836: $568 \pm 18 \text{ BP}$

$F^{14}\text{C} = 0.9317 \pm 0.0021$

$\delta^{13}\text{C} = 1.75 \text{ ‰ VPDB}$



485 Collection date: 1910
Collector: Mission Gruvel
Museum label: Mossamédès, m Gruvel, 1910

3.2 West African marine reservoir ages

490 The vast majority of the calculated ΔR values, with an average of -77 ± 47 ^{14}C yrs (1sd, $n = 25$), which corresponds to an averaged R value of 400 ± 59 ^{14}C yrs (1sd, $n = 25$), are typical of low latitudes marine reservoir age values (Bard, 1988; Bard et al., 1994) (Table S1 in the Supplement, Fig. 1). Our results agree perfectly with those already obtained (Ndeye, 2008) from the Nouadhibou-Cansado Bay area (Mauritania; Nh in Fig. 1) and the Dakar area (Senegal; Dk in Fig. 1); the only two areas that we can compare our results to.

495 No significant interspecific differences were observed. This is best illustrated for the localities where reservoir age values were obtained from at least two different species for the same calendar time. In the Dakar area (Senegal; Dk in Fig. 1) for years 1908-1909, we present data for 5 species (*Bucardium ringens*, *Donax rugosus*, *Mactra glabrata*, *Ostrea stentina*, *Senilia senilis*) (Ndeye, 2008; this study) all clustering within a range of [413;546] ([min; max]) with an average ΔR value of -16 ± 56 ^{14}C yrs (1sd, $n = 6$) (corresponding to an average R value of 478 ± 55 ^{14}C yrs). This was also the case for Luanda (Angola; Lu in Fig. 1) in the year 1910, with two species (*Donax rugosus* and *Senilia senilis*) yielding the same reservoir age values.
500 This was further supported for the area of Nouadhibou-Cansado Bay (Mauritania) showing the same pattern (Ndeye, 2008; this study), although one sample over four was likely an outlier (*Bucardium ringens* with # MNHN-IM-2022-4599). The fact that species living in very different ecological habitats (e.g., *Senilia senilis* in lagoons/semi-enclosed bays and *Donax rugosus* on beaches exposed to heavy surf; see also section material) show similar reservoir age values (R or ΔR) suggests that the habitat only exerts a minor influence on measured reservoir age. The fact that all investigated species in this study correspond
505 to suspension feeders further implies that suspension feeders are suitable material for reservoir age reconstruction.

Unlike semi-isolated basins such as the Black Sea (Soulet et al., 2019), where the radiocarbon system is closely linked to the local carbon stable isotopic system, the open-ocean coastal region of West Africa is characterized by the lack of any relationship between reservoir age values (R or ΔR) and stable oxygen and carbon isotope compositions (r^2 of 0.02 and 0.001, respectively), as inferred from our results.

510 3.3 Marine reservoir evolution over time

The local marine reservoir age were averaged over 5-yr windows ([1886-1890]-[1891-1895] and so on), excluding the five outliers discussed in section 3.5. Sample with radiocarbon lab # AA-70015 (see Table S1 in the Supplement) is a single value from 1916 and was averaged with samples from years 1912. We also calculated global marine reservoir age as the difference between the Marine20 and IntCal20 calibration curves. The evolution of the marine reservoir age of coastal West Africa (pink symbols in Fig. 2) shows a similar trend as that of the global marine reservoir age (black line in Fig. 2) with values declining
515 steadily with time since ca. 1900 AD. The ^{14}C age evolution of the global ocean (Marine20 calibration curve; Heaton et al.,



2020) is constructed using the global carbon cycle model BICYCLE (Köhler et al., 2006; Köhler and Fischer, 2006, 2004; Köhler et al., 2005). This box model incorporates a globally averaged atmospheric box and modules of the terrestrial (7 boxes) and oceanic (10 boxes) components of the carbon cycle. It is driven by temporal changes in the boundary conditions mimicking
520 changing climate and simulates changes in the carbon cycle including ^{14}C . To construct the Marine20 calibration curve, the BICYCLE model was revised to allow the atmospheric CO_2 and F^{14}C to be specified externally (Heaton et al., 2020). The global marine reservoir age evolution calculated as the difference between Marine20 and Intcal20 calibration curves (Fig.1) is thus also an output of the revised BICYCLE model. The fact that the trend in our measured marine reservoir age is similar to that of the globally modelled ones strongly suggest that global carbon cycle and climate are the first order drivers of the coastal
525 West African marine reservoir age rather than local effects.

3.4 Marine reservoir age off equatorial Ogooué and Congo rivers

Large rivers draining equatorial Africa as the Ogooué and Congo rivers inject massive amounts of freshwater into the Atlantic Ocean (Lambert et al., 2015; Milliman and Farnsworth, 2011) leading to extensive sea surface salinity negative anomalies (Martins and Stammer, 2022). The sea surface salinity negative anomalies are associated with net primary productivity positive
530 anomalies that are likely caused by the nutrient-rich river plumes from the Ogooué and Congo Rivers (Martins and Stammer, 2022). From a radiocarbon perspective, such net primary productivity positive anomalies should imply an increased uptake of atmospheric CO_2 through intensified biological pump. As a result, the reservoir age should be lower than average. The Congo River represents the second largest supplier of dissolved organic carbon (DOC) to global ocean with ~5% of the land to ocean DOC flux (Spencer et al., 2016; Coynel et al., 2005; Richey et al., 2022). The DOC exported by the Congo river is ^{14}C -modern
535 (Marwick et al., 2015; Spencer et al., 2012) and experiments showed that 45 % of the Congo River DOC can be photo-mineralized by sunlight (Spencer et al., 2009; Richey et al., 2022). Dissolved inorganic carbon (DIC) released from the photo-mineralisation of the Congo River DOC should also be ^{14}C -modern. Thus, this modern DOC-derived DIC should impact the marine reservoir age towards values lower compared to average. There is a lack of available data to estimate the age and flux of dissolved CO_2 discharged by the Congo river into the ocean (Richey et al., 2022). Nevertheless, the marine reservoir age
540 value measured at Port-Gentil (Gabon) close to the Ogooué river outlet is lower than average value ($\Delta R = -106 \pm 63$ ^{14}C years, corresponding to $R = 329 \pm 21$ ^{14}C yrs) (PG in Fig. 1). The marine reservoir age measured in Pointe-Noire (Republic of Congo) ~150 km north of the Congo river outlet is also lower than average ($\Delta R = -156 \pm 64$ ^{14}C yrs; $R = 289 \pm 20$ ^{14}C yrs) (PN in Fig. 1). These values could be interpreted as having been influenced by the Ogooué and Congo Rivers discharges. However, all other localities close to the Congo River outlet had marine reservoir age close to the average (Lo, Ca and Lu, in Fig. 1). Instead
545 the lower values observed in Port-Gentil (Gabon) and Pointe-Noire (Republic of Congo) are from years 1948 and 1937 suggesting that these lower values are in line with the declining global marine reservoir evolution linked to global climate and carbon cycle changes (see section 3.3). The impact of the African equatorial rivers on the local/regional coastal marine reservoir age, if any, cannot be inferred from our results.



3.5 Outlier specimens

550 Mean marine reservoir age values (R and ΔR) are provided for West Africa based on our data, excluding 5 samples. These
particular samples display much larger values with ΔR values ranging from 209 to 454 ^{14}C yrs or R values ranging from 701
to 912 ^{14}C yrs. Three specimens out of the five outlier samples correspond to *Bucardium ringens* specimens. We analysed 8
Bucardium ringens specimens. These 3 outlier specimens display reservoir age (R and ΔR) values that clearly disagree with
neighbouring data (Nouadhibou-Cansado Bay, Loos Islands and Ivory Coast areas; Nh, LI and IC in Fig. 1). The Museum
555 number of these specimens are MNHN-IM-2022-4597, MNHN-IM-2022-4599 and MNHN-IM-2022-4601. We do not expect
that these larger values compared to those for neighbouring individuals come from the species feeding practice as they are all
suspension feeders like all other investigated specimens. Similarly, we showed that the difference in the habitat does not impact
the specie reservoir ages. Instead *Bucardium ringens* lives in the open coast from 5-10 meters to about 50 meters depth. Shells
are commonly cast ashore on beaches but live-taken specimens are rare (von Cosel and Gofas, 2019). Two of the samples that
560 are outlier were collected at low tide (Roume Island in the Loos Islands; Republic of Guinea) or on a beach (Jacqueville; Ivory
Coast). It is thus possible that these outlier samples were transported subfossil samples that died a century or more before
collection date. Nevertheless, we cannot fully rule out that these higher values represent some variability in the local marine
reservoir age. Although, five *Bucardium ringens* samples out of eight displayed reservoir age values in agreement with the
neighbouring reservoir age values, this specie might not be the best suited for reservoir age reconstruction or for
565 sediment/archaeologic dating.

The two remaining outliers are *Ostrea stentina* specimens from the El Jadida area (Morocco; eJ in Fig. 1). The sample from
El Jadida beach was a single valve looking fresh and collected from the beach (museum # MNHN-IM-2022-4609). Based on
the older ^{14}C age of this specimen, we cannot rule out that this sample could actually be a subfossil specimen. The specimen
with museum # MNHN-IM-2022-4608 collected in the Sidi Moussa lagoon (south of El Jadida) was a specimen with the
570 articulated valves and remains of flesh was still inside the shell, meaning the specimen was still alive when collected. Variations
in the reservoir age could be explained by coastal upwelling that impacts some regions of the Atlantic coast of Morocco and
Western Sahara (Freudenthal et al., 2001; Barton et al., 1998). Upwelled waters can be depleted in ^{14}C relative to the sea
surface potentially causing larger reservoir age values (R or ΔR) like off Portugal (Monge Soares, 1993; Monge Soares and
Alveirinho Dias, 2006), California (Kennett et al., 1997), or Southern Arabian coast (Southon et al., 2002). Conversely,
575 upwelled waters can also be nutrient-rich causing intensified ocean CO_2 uptake through enhanced primary production and
biological pump (Williams and Follows, 2011), in that case, one could expect low-latitude average or decreased reservoir age
values (R or ΔR). Off Morocco and Western Sahara, the second hypothesis appears most likely as coastal upwelling in this
area is known to bring nutrient-rich waters to the surface ocean (Barton et al., 1998; Freudenthal et al., 2001), although to our
knowledge no direct measurement of the ^{14}C content of coastal waters in this region has been published yet. However,
580 according to recent studies the El Jadida area is only weakly impacted by upwelling (Lourenço et al., 2020; Cropper et al.,
2014), suggesting average reservoir age values instead of larger ones. Another explanation could be linked to the local



hydrology of the Sidi Moussa lagoon. Despite the lagoon is permanently connected to the ocean, it receives waters from rainfall and resurgences that can have an impact on the salinity in the upstream section of the lagoon (Cheggour et al., 2001). As the surrounding rocks are calcareous sandstones (Manaan, 2003), one could hypothesise that freshwaters feeding the lagoon might
585 be depleted in ^{14}C due to carbonate dissolution in the lagoon watershed causing a hardwater effect and thus a larger reservoir age. A last explanation could be due to an imperfect cleaning of the shell. For *Ostrea stentina*, sediment can be trapped between the growing layers of the shell. If this sediment contains old detrital carbonates and was not perfectly removed before ^{14}C measurement, the ^{14}C age of the shell will appear older, and the reservoir age larger. Additional reservoir age reconstructions from this region on different species would be require to validate the larger reservoir age values reconstructed from the El
590 Jadida area.

4 Conclusion

The analysis of pre-bomb suspension-feeding bivalves collected along coastal West Africa from 33°N to 15°S provides marine reservoir ages that are quite homogenous, with a mean ΔR value of -77 ± 47 ^{14}C yrs (1sd, $n = 25$) and a mean R value of 400 ± 59 ^{14}C yrs (1sd, $n = 25$). When including the robust dataset from Ndeye (2008), the resulting mean ΔR and R values for
595 coastal West Africa are -62 ± 51 ^{14}C years (1sd, $n = 33$) and 416 ± 61 ^{14}C years (1sd, $n = 33$), respectively. We show that the marine reservoir age of coastal West Africa is mainly driven by the global carbon cycle and climate rather than by local effects. Our results for different species yield similar marine reservoir age values, indicating that the ecological habitat only has a second-order impact on the reservoir age reconstruction, if any. Nevertheless, we suspect that *Bucardium ringens* might not be best suited for marine reservoir age reconstruction as corresponding shells are typically not found alive on sample collecting
600 sites. Additionally, ages obtained on *Ostrea stentina* could be possibly influenced by the presence of sediment within the growing shell layers if not fully removed after the cleaning process.

Despite these new data, large portions of the West African coast still remain to be investigated for reservoir age reconstructions, in particular off Western Sahara and Canarias Islands, Sierra Leone-Liberia, Nigeria and Namibia.

Author contribution statement

605 GSoulet designed the study and raised the funding. SG, PM, GSoulet and GSiani selected the specimens in the MNHN collections. GSoulet carried out the sample preparation with assistance of ML and FF. FD performed stable isotopes measurements. GSoulet performed reservoir calculations and analysed and discussed the data with GB, GSiani and SG. GSoulet wrote the manuscript with inputs from all co-authors.



Acknowledgements

610 We are grateful to the Muséum National d'Histoire Naturelle (Paris, France) for providing the samples. We thank the LMC14 staff (Laboratoire de Mesure du Carbone-14) and the CNRS-INSU ARTEMIS national radiocarbon AMS facility for providing radiocarbon measurements published in this study. The study was funded by the French national program INSU-LEFE (ResWA project – Pre-bomb Reservoir ages for the Western coast of Africa). I (GS) thank Ifremer in Brest and Sète for supporting my research. Finally, this study was carried out and the paper written during my part-time parental leave. I dedicate
615 this article to Marian, with whom I have had a wonderful time during this year, growing up together, him as a toddler and me as a father.

Competing interests

The authors declare that they have no conflict of interest.

Data availability

620 All data present in the paper are available in the text section 3.1 and in Table S1 in the Supplement.

References

- Alves, E. Q., Macario, K., Ascough, P., and Bronk Ramsey, C.: The worldwide marine radiocarbon reservoir effect: Definitions, mechanisms, and prospects, *Rev. Geophys.*, 56, 278–305, <https://doi.org/10.1002/2017RG000588>, 2018.
- Alves, E. Q., Macario, K. D., Urrutia, F. P., Cardoso, R. P., and Bronk Ramsey, C.: Accounting for the marine reservoir effect
625 in radiocarbon calibration, *Quat. Sci. Rev.*, 209, 129–138, <https://doi.org/10.1016/j.quascirev.2019.02.013>, 2019.
- Ascough, P., Cook, G., and Dugmore, A.: Methodological approaches to determining the marine radiocarbon reservoir effect, *Prog. Phys. Geogr. Earth Environ.*, 29, 532–547, <https://doi.org/10.1191/0309133305pp461ra>, 2005.
- Bard, E.: Correction of accelerator mass spectrometry ^{14}C ages measured in planktonic foraminifera: Paleooceanographic implications, *Paleoceanography*, 3, 635–645, <https://doi.org/10.1029/PA003i006p00635>, 1988.
- 630 Bard, E., Arnold, M., Mangerud, J., Paterne, M., Labeyrie, L., Duprat, J., Mélières, M.-A., Sønstegaard, E., and Duplessy, J.-C.: The North Atlantic atmosphere-sea surface ^{14}C gradient during the Younger Dryas climatic event, *Earth Planet. Sci. Lett.*, 126, 275–287, [https://doi.org/10.1016/0012-821X\(94\)90112-0](https://doi.org/10.1016/0012-821X(94)90112-0), 1994.
- Barton, E. D., Arístegui, J., Tett, P., Cantón, M., García-Braun, J., Hernández-León, S., Nykjaer, L., Almeida, C., Almunia, J., Ballesteros, S., Basterretxea, G., Escánez, J., García-Weill, L., Hernández-Guerra, A., López-Laatzén, F., Molina, R., Montero,
635 M. F., Navarro-Pérez, E., Rodríguez, J. M., van Lenning, K., Vélez, H., and Wild, K.: The transition zone of the Canary Current upwelling region, *Prog. Oceanogr.*, 41, 455–504, [https://doi.org/10.1016/S0079-6611\(98\)00023-8](https://doi.org/10.1016/S0079-6611(98)00023-8), 1998.



- Boettger, C. R.: Zur Molluskenfauna des Kongogebiets, *Ann. la Société R. Zool. Malacol. Belgique*, 47, 89–117, 1912.
- Boettger, O.: Katalog der Reptilien-Sammlung im Museum der Senckenbergischen Naturforschenden Gesellschaft in Frankfurt am Main, II Teil (Schlangen), Gebrüder Knauer, Frankfurt am Main, 1898.
- 640 Butzin, M., Köhler, P., and Lohmann, G.: Marine radiocarbon reservoir age simulations for the past 50,000 years, *Geophys. Res. Lett.*, 44, 8473–8480, <https://doi.org/10.1002/2017GL074688>, 2017.
- Catry, T., Figueira, P., Carvalho, L., Monteiro, R., Coelho, P., Lourenço, P. M., Catry, P., Tchantchalam, Q., Catry, I., Botelho, M. J., Pereira, E., Granadeiro, J. P., and Vale, C.: Evidence for contrasting accumulation pattern of cadmium in relation to other elements in *Senilia senilis* and *Tagelus adansonii* from the Bijagós archipelago, Guinea-Bissau, *Environ. Sci. Pollut. Res.*,
- 645 24, 24896–24906, <https://doi.org/10.1007/s11356-017-9902-8>, 2017.
- Cheggour, M., Chafik, A., Langston, W. ., Burt, G. ., Benbrahim, S., and Texier, H.: Metals in sediments and the edible cockle *Cerastoderma edule* from two Moroccan Atlantic lagoons: Moulay Bou Selham and Sidi Moussa, *Environ. Pollut.*, 115, 149–160, [https://doi.org/10.1016/S0269-7491\(01\)00117-8](https://doi.org/10.1016/S0269-7491(01)00117-8), 2001.
- von Cosel, R. and Gofas, S.: *Marine Bivalves of Tropical West Africa: From Rio de Oro to Southern Angola*, edited by:
- 650 MNHN and IRD, *Faune et Flore tropicales*, 48, Paris, Marseille, 1104 pp., 2019.
- Cottureau, E., Arnold, M., Moreau, C., Baqué, D., Bavay, D., Caffy, I., Comby, C., Dumoulin, J.-P., Hain, S., Perron, M., Salomon, J., and Setti, V.: Artemis, the new ¹⁴C AMS at LMC14 in Saclay, France, *Radiocarbon*, 49, 291–299, <https://doi.org/10.1017/S0033822200042211>, 2007.
- Coyne, A., Seyler, P., Etcheber, H., Meybeck, M., and Orange, D.: Spatial and seasonal dynamics of total suspended sediment
- 655 and organic carbon species in the Congo River, *Global Biogeochem. Cycles*, 19, n/a-n/a, <https://doi.org/10.1029/2004GB002335>, 2005.
- Cropper, T. E., Hanna, E., and Bigg, G. R.: Spatial and temporal seasonal trends in coastal upwelling off Northwest Africa, 1981–2012, *Deep Sea Res. Part I Oceanogr. Res. Pap.*, 86, 94–111, <https://doi.org/10.1016/j.dsr.2014.01.007>, 2014.
- Dautzenberg, P.: Mission Gruvel sur la côte occidentale d'Afrique (1909-1910): Mollusques marins. *Annales de l'Institut Océanographique*, Paris (Nouvelle Série). 5(3): 1-111, pl. 1-3, 1912.
- Dewar, G., Reimer, P. J., Sealy, J., and Woodborne, S.: Late-Holocene marine radiocarbon reservoir correction (ΔR) for the west coast of South Africa, *The Holocene*, 22, 1481–1489, <https://doi.org/10.1177/0959683612449755>, 2012.
- Dumoulin, J.-P., Comby-Zerbino, C., Delqué-Količ, E., Moreau, C., Caffy, I., Hain, S., Perron, M., Thellier, B., Setti, V., Berthier, B., and Beck, L.: Status report on sample preparation protocols developed at the LMC14 laboratory, Saclay, France:
- 665 From Sample Collection to ¹⁴C AMS Measurement, *Radiocarbon*, 59, 713–726, <https://doi.org/10.1017/RDC.2016.116>, 2017.
- Freudenthal, T., Neuer, S., Meggers, H., Davenport, R., and Wefer, G.: Influence of lateral particle advection and organic matter degradation on sediment accumulation and stable nitrogen isotope ratios along a productivity gradient in the Canary Islands region, *Mar. Geol.*, 177, 93–109, [https://doi.org/10.1016/S0025-3227\(01\)00126-8](https://doi.org/10.1016/S0025-3227(01)00126-8), 2001.
- Heaton, T. J., Köhler, P., Butzin, M., Bard, E., Reimer, R. W., Austin, W. E. N., Bronk Ramsey, C., Grootes, P. M., Hughen, K. A., Kromer, B., Reimer, P. J., Adkins, J., Burke, A., Cook, M. S., Olsen, J., and Skinner, L. C.: Marine20—The Marine
- 670

Radiocarbon Age Calibration Curve (0–55,000 cal BP), *Radiocarbon*, 62, 779–820, <https://doi.org/10.1017/RDC.2020.68>, 2020.

675 Heaton, T. J., Bard, E., Bronk Ramsey, C., Butzin, M., Köhler, P., Muscheler, R., Reimer, P. J., and Wacker, L.: Radiocarbon: A key tracer for studying Earth's dynamo, climate system, carbon cycle, and Sun, *Science* (80-.), 374, <https://doi.org/10.1126/science.abd7096>, 2021.

Heaton, T. J., Bard, E., Bronk Ramsey, C., Butzin, M., Hatté, C., Hughen, K. A., Köhler, P., and Reimer, P. J.: A response to community questions on the Marine20 radiocarbon age calibration curve: Marine reservoir ages and the calibration of ^{14}C samples from the oceans, *Radiocarbon*, 65, 247–273, <https://doi.org/10.1017/RDC.2022.66>, 2023.

680 Herrera, N. D., ter Poorten, J. J., Bieler, R., Mikkelsen, P. M., Strong, E. E., Jablonski, D., and Stepan, S. J.: Molecular phylogenetics and historical biogeography amid shifting continents in the cockles and giant clams (Bivalvia: Cardiidae), *Mol. Phylogenet. Evol.*, 93, 94–106, <https://doi.org/10.1016/j.ympev.2015.07.013>, 2015.

Hogg, A. G., Heaton, T. J., Hua, Q., Palmer, J. G., Turney, C. S., Southon, J., Bayliss, A., Blackwell, P. G., Boswijk, G., Bronk Ramsey, C., Pearson, C., Petchey, F., Reimer, P., Reimer, R., and Wacker, L.: SHCal20 Southern Hemisphere Calibration, 0–55,000 Years cal BP, *Radiocarbon*, 62, 759–778, <https://doi.org/10.1017/RDC.2020.59>, 2020.

685 Kennett, D. J., Ingram, B. L., Erlandson, J. M., and Walker, P.: Evidence for Temporal Fluctuations in Marine Radiocarbon Reservoir Ages in the Santa Barbara Channel, Southern California, *J. Archaeol. Sci.*, 24, 1051–1059, <https://doi.org/10.1006/jasc.1996.0184>, 1997.

Köhler, P. and Fischer, H.: Simulating changes in the terrestrial biosphere during the last glacial/interglacial transition, *Glob. Planet. Change*, 43, 33–55, <https://doi.org/10.1016/j.gloplacha.2004.02.005>, 2004.

690 Köhler, P. and Fischer, H.: Simulating low frequency changes in atmospheric CO_2 during the last 740 000 years, *Clim. Past*, 2, 57–78, <https://doi.org/10.5194/cp-2-57-2006>, 2006.

Köhler, P., Fischer, H., Munhoven, G., and Zeebe, R. E.: Quantitative interpretation of atmospheric carbon records over the last glacial termination, *Global Biogeochem. Cycles*, 19, n/a-n/a, <https://doi.org/10.1029/2004GB002345>, 2005.

695 Köhler, P., Muscheler, R., and Fischer, H.: A model-based interpretation of low-frequency changes in the carbon cycle during the last 120,000 years and its implications for the reconstruction of atmospheric $\Delta^{14}\text{C}$, *Geochemistry, Geophys. Geosystems*, 7, n/a-n/a, <https://doi.org/10.1029/2005GC001228>, 2006.

Lambert, T., Darchambeau, F., Bouillon, S., Alhou, B., Mbega, J.-D., Teodoru, C. R., Nyoni, F. C., Massicotte, P., and Borges, A. V.: Landscape control on the spatial and temporal variability of chromophoric dissolved organic matter and dissolved organic carbon in large African Rivers, *Ecosystems*, 18, 1224–1239, <https://doi.org/10.1007/s10021-015-9894-5>, 2015.

700 Lindsay, C. M., Lehman, S. J., Marchitto, T. M., Carriquiry, J. D., and Ortiz, J. D.: New constraints on deglacial marine radiocarbon anomalies from a depth transect near Baja California, *Paleoceanography*, 31, 1103–1116, <https://doi.org/10.1002/2015PA002878>, 2016.

Lourenço, C. R., Nicastro, K. R., McQuaid, C. D., Krug, L. A., and Zardi, G. I.: Strong upwelling conditions drive differences in species abundance and community composition along the Atlantic coasts of Morocco and Western Sahara, *Mar. Biodivers.*,



- 705 50, 15, <https://doi.org/10.1007/s12526-019-01032-z>, 2020.
- Mana'an, M.: Étude sédimentologique du remplissage de la lagune de Sidi Moussa, Maroc, PhD thesis, Université Chouaib Doukkali, El Jadida, <https://theses.hal.science/tel-00124571>, 2003.
- Martins, M. S. and Stammer, D.: Interannual variability of the Congo River plume-induced sea surface salinity, *Remote Sens.*, 14, 1013, <https://doi.org/10.3390/rs14041013>, 2022.
- 710 Marwick, T. R., Tamoo, F., Teodoru, C. R., Borges, A. V., Darchambeau, F., and Bouillon, S.: The age of river-transported carbon: A global perspective, *Global Biogeochem. Cycles*, 29, 122–137, <https://doi.org/10.1002/2014GB004911>, 2015.
- Milliman, J. D. and Farnsworth, K. L.: *River discharge to the coastal ocean*, Cambridge University Press, <https://doi.org/10.1017/CBO9780511781247>, 2011.
- Monge Soares, A.: The ^{14}C content of marine shells: Evidence for variability in coastal upwelling off Portugal during the
715 Holocene, in: *Isotope techniques in the study of past and current environmental changes in the hydrosphere and the atmosphere proceedings*, edited by: IAEA, Vienna, 471–485, 1993.
- Monge Soares, A. M. and Alveirinho Dias, J. M.: Coastal upwelling and radiocarbon-evidence for temporal fluctuations in ocean reservoir effect off Portugal during the holocene, *Radiocarbon*, 48, 45–60, <https://doi.org/10.1017/S0033822200035384>, 2006.
- 720 Mook, W. G. and van der Plicht, J.: Reporting ^{14}C activities and concentrations, *Radiocarbon*, 41, 227–239, <https://doi.org/10.1017/S0033822200057106>, 1999.
- Moreau, C., Caffy, I., Comby, C., Delqué-Količ, E., Dumoulin, J.-P., Hain, S., Quiles, A., Setti, V., Souprayen, C., Thellier, B., and Vincent, J.: Research and development of the Artemis ^{14}C AMS facility: Status report, *Radiocarbon*, 55, 331–337, <https://doi.org/10.1017/S0033822200057441>, 2013.
- 725 Ndeye, M.: Marine reservoir ages in Northern Senegal and Mauritania coastal waters, *Radiocarbon*, 50, 281–288, <https://doi.org/10.1017/S0033822200033580>, 2008.
- Okera, W.: Observations on some population parameters of exploited stocks of *Senilia senilis* (= *Arca senilis*) in Sierra Leone, *Mar. Biol.*, 38, 217–229, <https://doi.org/10.1007/BF00388935>, 1976.
- Oliver, P. G. and von Cosel, R.: Taxonomy of tropical west African Bivalves. IV. Arcidae., *Bull. Muséum Natl. d'Histoire
730 Nat.*, 14, 293–381, 1992.
- Reimer, P. J. and McCormac, F. G.: Marine radiocarbon reservoir corrections for the Mediterranean and Aegean Seas, *Radiocarbon*, 44, 159–166, <https://doi.org/10.1017/S0033822200064766>, 2002.
- Reimer, P. J. and Reimer, R. W.: A marine reservoir correction database and on-line interface, *Radiocarbon*, 43, 461–463, <https://doi.org/10.1017/S0033822200038339>, 2001.
- 735 Reimer, P. J., Brown, T. A., and Reimer, R. W.: Discussion: Reporting and calibration of post-bomb ^{14}C data, *Radiocarbon*, 46, 1299–1304, <https://doi.org/10.1017/S0033822200033154>, 2004.
- Reimer, P. J., Austin, W. E. N., Bard, E., Bayliss, A., Blackwell, P. G., Bronk Ramsey, C., Butzin, M., Cheng, H., Edwards, R. L., Friedrich, M., Grootes, P. M., Guilderson, T. P., Hajdas, I., Heaton, T. J., Hogg, A. G., Hughen, K. A., Kromer, B.,



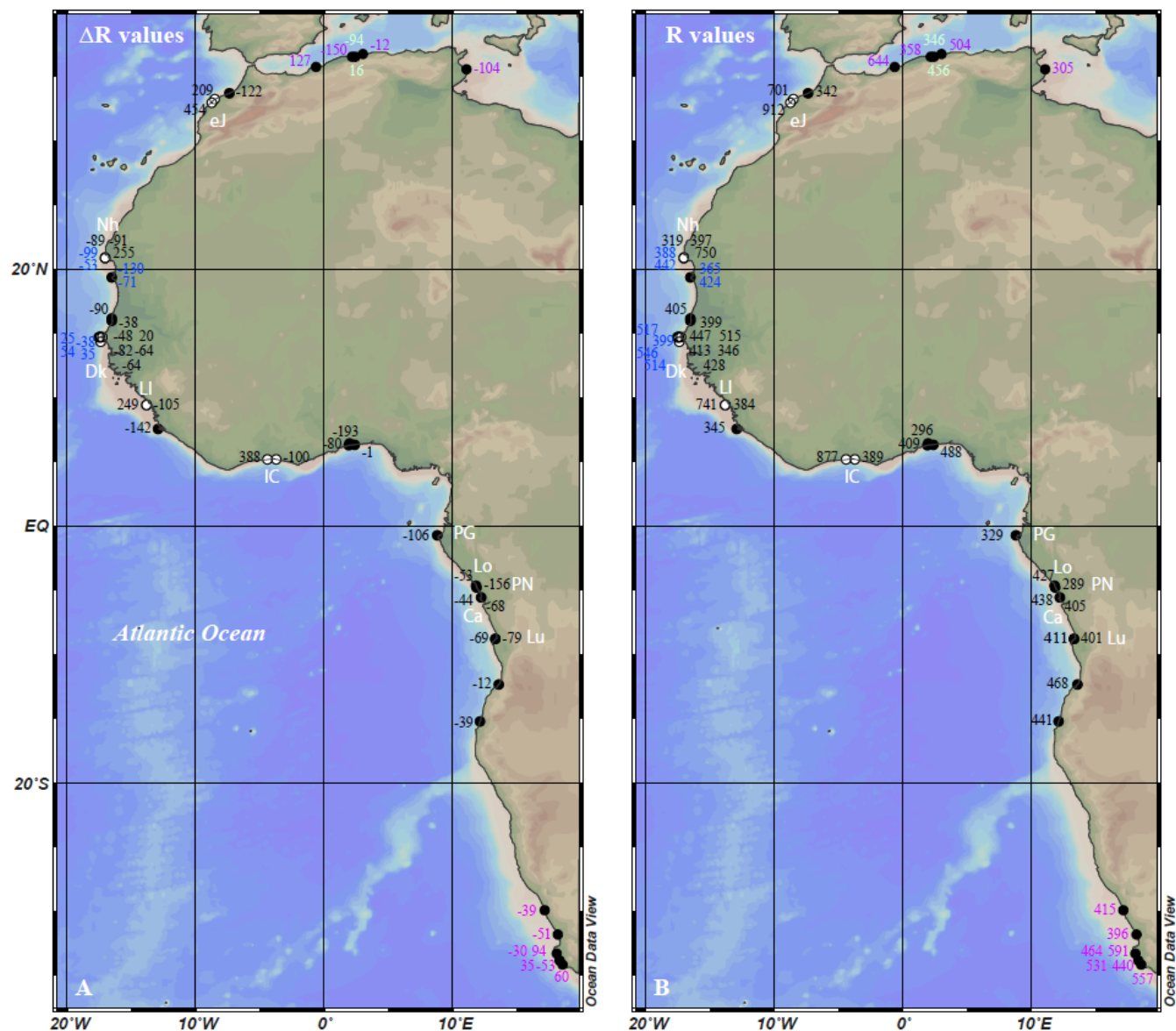
- Manning, S. W., Muscheler, R., Palmer, J. G., Pearson, C., van der Plicht, J., Reimer, R. W., Richards, D. A., Scott, E. M.,
740 Southon, J. R., Turney, C. S. M., Wacker, L., Adolphi, F., Büntgen, U., Capano, M., Fahrni, S. M., Fogtman-Schulz, A.,
Friedrich, R., Köhler, P., Kudsk, S., Miyake, F., Olsen, J., Reinig, F., Sakamoto, M., Sookdeo, A., and Talamo, S.: The IntCal20
northern hemisphere radiocarbon age calibration curve (0–55 cal kBP), *Radiocarbon*, 62, 725–757,
<https://doi.org/10.1017/RDC.2020.41>, 2020.
- Reimer, R. W. and Reimer, P. J.: An online application for ΔR calculation, *Radiocarbon*, 59, 1623–1627,
745 <https://doi.org/10.1017/RDC.2016.117>, 2017.
- Richey, J. E., Spencer, R. G. M., Drake, T. W., and Ward, N. D.: Fluvial carbon dynamics across the land to ocean continuum
of great tropical rivers, 391–412, <https://doi.org/10.1002/9781119657002.ch20>, 2022.
- Roux, C.: Compte rendu sommaire d’une mission en Afrique Équatoriale Française, *Bull. du Muséum Natl. d’Histoire Nat.*,
21, 500–503, 1949.
- 750 Santos, G. M., Southon, J. R., Griffin, S., Beaupre, S. R., and Druffel, E. R. M.: Ultra small-mass AMS ^{14}C sample preparation
and analyses at KCCAMS/UCI Facility, *Nucl. Instruments Methods Phys. Res. Sect. B Beam Interact. with Mater. Atoms*,
259, 293–302, <https://doi.org/10.1016/j.nimb.2007.01.172>, 2007.
- Schefeuf, E., Eglinton, T. I., Spencer-Jones, C. L., Rullkötter, J., De Pol-Holz, R., Talbot, H. M., Grootes, P. M., and Schneider,
R. R.: Hydrologic control of carbon cycling and aged carbon discharge in the Congo River basin, *Nat. Geosci.*, 9, 687–690,
755 <https://doi.org/10.1038/ngeo2778>, 2016.
- Sessa, J. A., Callapez, P. M., Dinis, P. A., and Hendy, A. J. W.: Paleoenviromental and paleobiogeographical implications of
a middle Pleistocene mollusc assemblage from the marine terraces of Baía Das Pipas, southwest Angola, *J. Paleontol.*, 87,
1016–1040, <https://doi.org/10.1666/12-119>, 2013.
- Siani, G., Paterne, M., Arnold, M., Bard, E., Métiévier, B., Tisnerat, N., and Bassinot, F.: Radiocarbon reservoir ages in the
760 Mediterranean Sea and Black Sea, *Radiocarbon*, 42, 271–280, <https://doi.org/10.1017/S0033822200059075>, 2000.
- Siani, G., Paterne, M., Michel, E., Sulpizio, R., Sbrana, A., Arnold, M., and Haddad, G.: Mediterranean Sea surface
radiocarbon reservoir age changes since the Last Glacial Maximum, *Science* (80-.), 294, 1917–1920,
<https://doi.org/10.1126/science.1063649>, 2001.
- Skinner, L., McCave, I. N., Carter, L., Fallon, S., Scrivner, A. E., and Primeau, F.: Reduced ventilation and enhanced
765 magnitude of the deep Pacific carbon pool during the last glacial period, *Earth Planet. Sci. Lett.*, 411, 45–52,
<https://doi.org/10.1016/j.epsl.2014.11.024>, 2015.
- Skinner, L. C. and Bard, E.: Radiocarbon as a dating tool and tracer in paleoceanography, *Rev. Geophys.*, 60, 1–64,
<https://doi.org/10.1029/2020RG000720>, 2022.
- Skinner, L. C., Fallon, S., Waelbroeck, C., Michel, E., and Barker, S.: Ventilation of the deep Southern Ocean and deglacial
770 CO_2 rise, *Science* (80-.), 328, 1147–1151, <https://doi.org/10.1126/science.1183627>, 2010.
- Smith, D. A. S.: Polymorphism and population density in *Donax rugosus* (Lamellibranchiata: Donacidae), *J. Zool.*, 164, 429–
441, <https://doi.org/10.1111/j.1469-7998.1971.tb01327.x>, 1971.



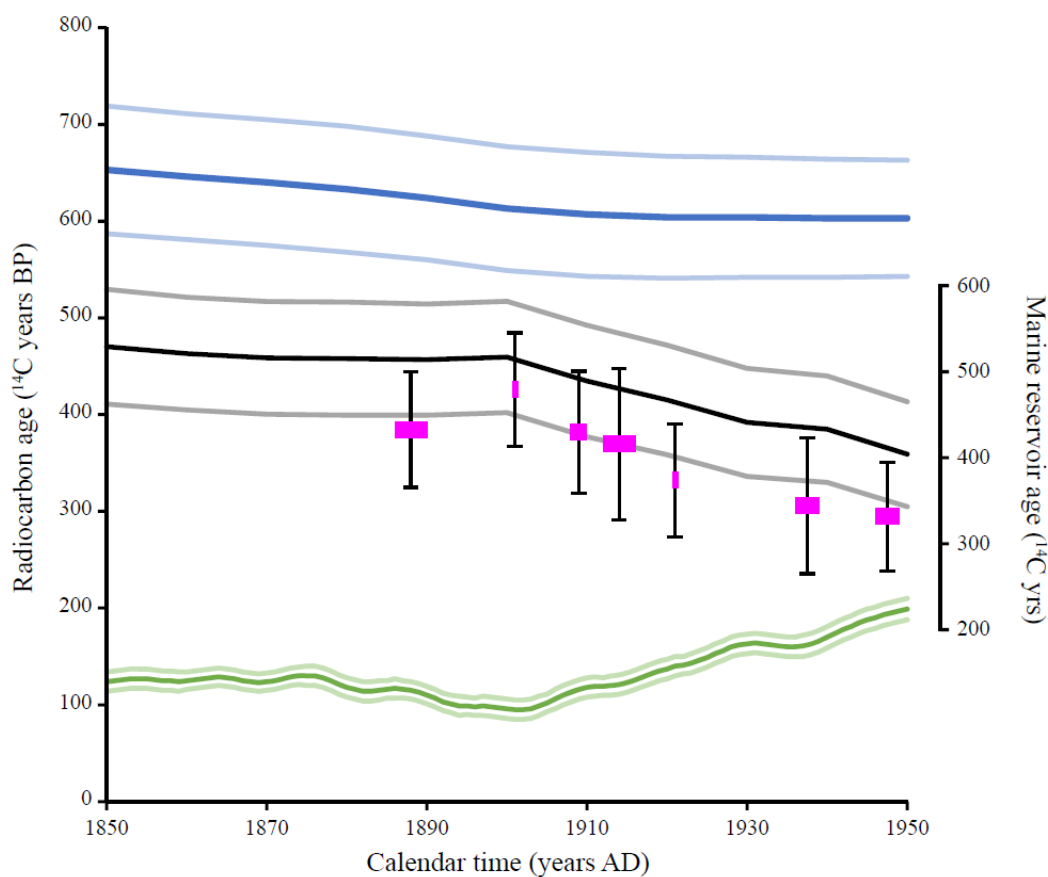
- Soulet, G.: Methods and codes for reservoir–atmosphere ^{14}C age offset calculations, *Quat. Geochronol.*, 29, 97–103, <https://doi.org/10.1016/j.quageo.2015.05.023>, 2015.
- 775 Soulet, G., Ménot, G., Garreta, V., Rostek, F., Zaragosi, S., Lericolais, G., and Bard, E.: Black Sea “Lake” reservoir age evolution since the Last Glacial — Hydrologic and climatic implications, *Earth Planet. Sci. Lett.*, 308, 245–258, <https://doi.org/10.1016/j.epsl.2011.06.002>, 2011.
- Soulet, G., Skinner, L. C., Beaupré, S. R., and Galy, V.: A note on reporting of reservoir ^{14}C disequilibria and age offsets, *Radiocarbon*, 58, 205–211, <https://doi.org/10.1017/RDC.2015.22>, 2016.
- 780 Soulet, G., Giosan, L., Flaux, C., and Galy, V.: Using stable carbon isotopes to quantify radiocarbon reservoir age offsets in the coastal black sea, *Radiocarbon*, 61, <https://doi.org/10.1017/RDC.2018.61>, 2019.
- Southon, J., Kashgarian, M., Fontugne, M., Metivier, B., and Yim, W. W. S.: Marine reservoir corrections for the Indian Ocean and Southeast Asia, *Radiocarbon*, 44, 167–180, <https://doi.org/10.1017/S0033822200064778>, 2002.
- Spencer, R. G. M., Stubbins, A., Hernes, P. J., Baker, A., Mopper, K., Aufdenkampe, A. K., Dyda, R. Y., Mwamba, V. L.,
785 Mangangu, A. M., Wabakanghanzi, J. N., and Six, J.: Photochemical degradation of dissolved organic matter and dissolved lignin phenols from the Congo River, *J. Geophys. Res.*, 114, G03010, <https://doi.org/10.1029/2009JG000968>, 2009.
- Spencer, R. G. M., Hernes, P. J., Aufdenkampe, A. K., Baker, A., Gulliver, P., Stubbins, A., Aiken, G. R., Dyda, R. Y., Butler, K. D., Mwamba, V. L., Mangangu, A. M., Wabakanghanzi, J. N., and Six, J.: An initial investigation into the organic matter biogeochemistry of the Congo River, *Geochim. Cosmochim. Acta*, 84, 614–627, <https://doi.org/10.1016/j.gca.2012.01.013>,
790 2012.
- Spencer, R. G. M., Hernes, P. J., Dinga, B., Wabakanghanzi, J. N., Drake, T. W., and Six, J.: Origins, seasonality, and fluxes of organic matter in the Congo River, *Global Biogeochem. Cycles*, 30, 1105–1121, <https://doi.org/10.1002/2016GB005427>, 2016.
- Stuiver, M. and Braziunas, T. F.: Modeling atmospheric ^{14}C influences and ^{14}C ages of marine samples to 10,000 BC, *Radiocarbon*, 35, 137–189, <https://doi.org/10.1017/S0033822200013874>, 1993.
- 795 Stuiver, M. and Polach, H. A.: Discussion: Reporting of ^{14}C Data, *Radiocarbon*, 19, 355–363, <https://doi.org/10.1017/S0033822200003672>, 1977.
- Stuiver, M., Pearson, G. W., and Braziunas, T.: Radiocarbon age calibration of marine samples back to 9000 cal yr BP, *Radiocarbon*, 28, 980–1021, <https://doi.org/10.1017/S0033822200060264>, 1986.
- 800 Tisnérat-Laborde, N., Poupeau, J. J., Tannau, J. F., and Paterne, M.: Development of a semi-automated system for routine preparation of carbonate samples, *Radiocarbon*, 43, 299–304, <https://doi.org/10.1017/S0033822200038145>, 2001.
- Türkmen, A., Türkmen, M., and Tepe, Y.: Biomonitoring of heavy metals from Iskenderun Bay using two bivalve species *Chama pacifica* Broderip, 1834 and *Ostrea stentina* Payraudeau, 1826, *Turkish J. Fish. Aquat. Sci.*, 5, 107–111, 2005.
- Westhoff, F.: Die Fauna der Kongo-Mündung, *Jahresbericht der Zool. Sekt. Westfälischen Prov. Vereins für Wiss. und Kunst für das Etatsjahr 1885-86*, 38–40, 1886.
- 805 Williams, R. G. and Follows, M. J.: *Ocean dynamics and the carbon cycle: Principles and mechanisms*, Cambridge.,



Cambridge, 434 pp., 2011.



810 Figure 1: The geographic distribution of marine reservoir age values along the West African coast. A. ΔR values. B. R values. Data
 shown in black are from this study. Other are selected results from previous studies discussed in the text, converted from their
 original format (conventional ^{14}C ages and collection dates) to ΔR and R values using the latest calibration curves Marine20 (Heaton
 et al., 2020) and Intcal20 or SHcal20 (Reimer et al., 2020; Hogg et al., 2020), respectively. Data in blue are from Ndeye (2008), data
 815 in green are from (Reimer and McCormac, 2002), data in purple are from (Siani et al., 2000) and data in pink are from (Dewar et
 al., 2012). ej, Nh, Dk, LI, IC and Lu stand for el Jadida (Morocco), Nouadhibou (Mauritania), Dakar (Senegal), Loos Islands
 (Republic of Guinea), Ivory Coast and Luanda (Angola). The map was drawn using Ocean Data View (Schlitzer, Reiner, Ocean
 Data View, <https://odv.awi.de>, 2022).



820 **Figure 2:** Left axis: The radiocarbon age evolution of the atmosphere (IntCal20; green curve with its light green 1- σ envelope) and of the global ocean (Marine20; blue curve with its light blue 1- σ envelope) between 1850 and 1950 AD. Right axis: The global marine reservoir age (black curve with its grey 1- σ envelope) calculated as the difference between Marine20 and Intcal20 curves. Pink symbols are the coastal West African marine reservoir age calculated averaging data over 5-yr windows. The reported error bars are the maximum of the standard deviation of the averaged data and the individual uncertainty of the averaged data.